Thermal Property, Structure, and Dynamics of Supercooled Water in Porous Silica by Calorimetry, Neutron Scattering, and NMR Relaxation

ARTICLE *in* THE JOURNAL OF PHYSICAL CHEMISTRY B · JULY 1997

Impact Factor: 3.3 · DOI: 10.1021/jp9631238

5 AUTHORS, INCLUDING:

Toshiyuki Takamuku
Saga University
84 PUBLICATIONS **1,928** CITATIONS

SEE PROFILE

Hisanobu Wakita
Fukuoka University
151 PUBLICATIONS **1,676** CITATIONS

SEE PROFILE

Toshio Yamaguchi
Fukuoka University
203 PUBLICATIONS **3,792** CITATIONS

SEE PROFILE

Thermal Property, Structure, and Dynamics of Supercooled Water in Porous Silica by Calorimetry, Neutron Scattering, and NMR Relaxation

Toshiyuki Takamuku,[†] Motoyuki Yamagami, Hisanobu Wakita, Yuichi Masuda,[‡] and Toshio Yamaguchi*

Department of Chemistry, Faculty of Science, Fukuoka University, Nanakuma, Jonan-ku, Fukuoka 814-80, Japan, and Department of Chemistry, Faculty of Science, Ochanomizu University, Bunkyo-ku, Tokyo 112, Japan

Received: October 10, 1996; In Final Form: April 12, 1997[⊗]

Thermal properties, structure, and dynamics of supercooled water in porous silica of two different pore sizes (30 and 100 Å) have been investigated over a temperature range from 298 down to 193 K by differential scanning calorimetry (DSC), neutron diffraction, neutron quasi-elastic scattering, and proton NMR relaxation methods. Cooling curves by DSC showed that water in the 30 Å pores freezes at around 237 K, whereas water in the 100 Å pores does at 252 K. Neutron diffraction data for water in the 30 Å pores revealed that with lowering temperatures below 237 K hydrogen bond networks are gradually strengthened, the structure correlation being extended to 10 Å at 193 K. It has also been found that crystalline ice is not formed in the 30 Å pores in the temperature range investigated, whereas cubic ice (I_c) crystallizes in the 100 Å pores at 238 K. The self-diffusion coefficients of water protons in both pores determined from the quasi-elastic neutron scattering measurements showed that the translational motion of water molecules is slower by a factor of two in the 30 Å pores than in the 100 Å pores, the motion of water molecules in the 100 Å pores being comparable with that of bulk water. The self-diffusion coefficients of water in both pores at different temperatures showed that the translational motion of water molecules is gradually restricted with decreasing temperature. The spin-lattice relaxation time (T_1) and the spin-spin relaxation time (T_2) data obtained by the proton NMR relaxation experiments suggested that the motions of water molecules in the 100 Å pores are faster by a factor of 2−3 than those of water molecules in the 30 Å pores. The peak area, the half-width at half maximum, the relaxation rates (T_1^{-1} and T_2^{-1}) of water molecules at the various temperatures all showed an inflection point at 238 and 253 K for the 30 and 100 Å pores, respectively, suggesting the freezing of water in the pores.

Introduction

The structure and dynamic properties of water in micropores are essential in understanding chemical reactions in catalysts, and chemical absorption and properties of ion exchange resins. Water in micropores of 20−100 Å in diameter is easily supercooled to a temperature around 233 K, in contrast with bulk water which can be supercooled to ∼260 K. Thus, investigations of the structure and dynamics of water in micropores give information about hydrogen bonds in supercooled water and a hint on nonfreezing water in living biological cells.

The properties of water in micropores such as porous silicas and polymer gels have been widely investigated by various methods.[1−24] Most of the early investigations before 1980 have been summarized in the literatures.[1−3] Hall and his co-workers[9] studied the dynamics of water molecules in porous silica, Spherisorb S20W, with a pore size of 90 Å at ambient temperature by inelastic neutron scattering and concluded that the vibrational energy of water molecules in the pores is lower than that of bulk water. They also performed dielectric relaxation experiments on water at the surface of the silica.[10] Clark *et al.*[11] studied the dynamics of water molecules in Spherisorb S20W by quasi-elastic neutron scattering and determined both translational and rotational diffusion coefficients of water molecules at ambient temperature. Steytler *et al.*[12] performed neutron diffraction measurements at 293 and 348 K on D_2O in Spherisorb S20W and Gasil 200 with a pore size of 20 Å. They found that the structure of water at the surface of silica is not significantly different from that of bulk water and that the silanol groups at the surface influence the structure of water to a distance of about 10 Å.

In spite of these efforts under ambient conditions, there are only a few reports on microscopic behaviors of water in micropores at undercooled temperatures.[10,15,22−24] Dore *et al.*[15] first measured neutron diffraction of D_2O in Spherisorb S20W at undercooled temperatures down to 213 K and preliminarily reported that ice I_h first crystallized at 260 K and transformed to ice I_c at around 252 K in the pores. The dynamics of water molecules in Spherisorb S7W (the pore size is 90 Å) at undercooled temperatures was discussed on the basis of proton NMR measurements by Hall *et al.*[10] Bellissent-Funel *et al.* recently investigated the structure[22] and dynamics[23] of water filled in Vycor 7930, which has 1.6 mm thickness, 32 × 36 mm^2 area, and 50 Å pore size, by neutron diffraction and quasi-elastic and inelastic neutron scattering. They found crystallization of ice I_c in the Vycor glass at 255 K from the neutron diffraction measurements. Their quasi-elastic scattering experiments showed that the values of the proton self-diffusion coefficient rapidly decrease as the temperature decreases,

* Author to whom all correspondence should be addressed.
[†] On leave from Aqua Laboratory, Research and Development Division, TOTO Ltd., Nakashima, Kokurakita-ku, Kitakyushu 802, Japan.
[‡] Ochanomizu University.
[⊗] Abstract published in *Advance ACS Abstracts,* June 1, 1997.

S1089-5647(96)03123-9 CCC: $14.00

revealing restricted translational motion of water molecules with lowering temperature. Hansen and his co-workers[24] have recently performed ^{1}H NMR measurements on water confined in some mesoporous materials such as MCM-41, whose pore radii are larger than 10 Å, at undercooled temperatures. On the basis of the observed NMR intensities, they found one or more pore size dependent transitions of water above 222 K and an additional transition below 209 K, which is independent of pore dimension. Furthermore, they have estimated the thickness of the interfacial water (5.4 ± 1.0 Å) between the matrix surface and the solid ice phase formed in the pore center. In spite of these efforts, there are no comprehensive investigations about both structure and dynamic properties of supercooled water in porous silicas with different pore sizes.

In the present study both microscopic structure and dynamic properties have been investigated for supercooled water in porous silicas with two different pore sizes of 30 and 100 Å over a temperature range of 193 to 298 K. First, the thermal behavior of water in both 30 and 100 Å pores has been examined by differential scanning calorimetry. Then, neutron diffraction measurements have been performed on water in the pores with lowering temperature to understand the structural change of water. Finally, both quasi-elastic neutron scattering and proton NMR relaxation experiments have been performed to study the dynamics of water molecules in the pores over a wide temperature range. The effect of the pore size on the properties of water is discussed on the basis of the results obtained.

Experimental Section

Preparation of Samples. Porous silicas, Develosils 30 and 100 (Nomura Chemicals Ltd.), have, respectively, a particle diameter of 3 mm, average pore diameters of 30 and 100 Å, surface areas of 650 and 350 m^2/g, and pore volume of 0.50 and 1.0 cm^3/g. The pores were filled up to about 12−100% of the volume with H_2O or D_2O by an evaporation method as follows. First, the silicas were dried over P_2O_5 in a vacuum desiccator for several days. The water content in the silicas was checked with a thermal gravimeter (Rigaku PTC-10A). The dried silica was then kept in a desiccator containing H_2O or D_2O (ISOTEC Inc. 99.9%) until the pores of the silica were filled with water to a required amount. The amount of water in the silicas was determined by thermal gravimetry to estimate the water content R (= the ratio of the observed moles of water to the theoretical moles of water filling the whole volume of pores). In preparation of samples for neutron diffraction measurements, the above procedure was repeated several times to replace the protons of silanol groups with deuterons.

Differential Scanning Calorimetry (DSC). DSC measurements were made on both silica samples filled with H_2O at various water contents using a differential scanning calorimeter (SEIKO I 5000). DSC curves for water in the silica was recorded first on cooling from 293 down to 173 K, and then on heating up to 293 K. Both cooling and heating rates were controlled at 2 K min^{-1}.

Neutron Diffraction Experiments. Time-of-flight (TOF) pulsed neutron diffraction measurements were made on a HIT instrument at a pulsed neutron facility (KENS) of the National Laboratory for High Energy Physics (KEK), Tsukuba. Details of HIT and its performance have been described elsewhere.[25] D_2O was used in neutron diffraction measurements to avoid large incoherent scatterings from the protons in H_2O. The measurements were carried out on D_2O in Develosils 30 and 100 at $R = 1.0$ and 0.76 and on bulk D_2O. A sample was kept in a cell made of a Ti−Zr null matrix alloy with 85 mm height, 8 mm inner diameter, and 0.3 mm wall thickness at required temperatures. The temperature of a sample was measured with an Au−0.07%Fe−Chromel thermocouple and controlled to within ±0.5 K. The temperatures measured were 193, 223, 243, 258, 275, and 295 K for a Develosil 30 sample, 213, 238, 248, and 295 K for a Develosil 100 sample, and 213 and 295 K for bulk D_2O. Prior to the measurements a sample was left at a temperature chosen for 30−60 min. The intensities of scattered neutrons were accumulated for about 10 and 1 h for the Develosils 30 and 100 samples, respectively. The scattering intensities of a dry silica sample, an empty cell, background, and a vanadium rod of 8 mm diameter were also measured at 295 K.

The observed scattering data for the samples and the empty cell were corrected for background, absorption,[26] and multiple[27] scattering. The contribution from D_2O, $I_W(Q)$, in the total scattering intensity of the silica samples was obtained by eq 1

$$I_W(Q) = [I_{SWC}(Q) - I_C(Q)] - f[I_S(Q) - I_C(Q)], \quad (1)$$

where the momentum transfer Q is given by $(4\pi/\lambda)\sin\theta$ with the scattering angle 2θ and the wavelength λ, $I_{SWC}(Q)$ is the corrected intensity of the silica sample containing D_2O, $I_C(Q)$ is the scattering of an empty Ti−Zr cell, $I_S(Q)$ is the intensity of the dry silica, and f is a factor. The factor f was calculated as $f = W_{S,SW}/W_{S,S}$, where $W_{S,SW}$ is the weight of silica in the sample, which was obtained by reduction of the weight of D_2O from the total weight of the sample, and $W_{S,S}$ is the weight of the dry silica. The corrected intensity $I_W(Q)$ was normalized to an absolute unit by use of the intensities of the vanadium rod.

The structure factor $S(Q)$ can be defined as

$$S(Q) = \frac{I_W(Q) - \sum b_i^2 + (\sum b_i)^2}{(\sum b_i)^2}, \quad (2)$$

where b_i is the coherent scattering length of the i-th nucleus, and their values were taken from the literature.[28] In order to clarify the change in structure of D_2O in Develosil 30 with temperature, the difference structure factor $\Delta S(Q)$ was derived on the basis of those measured at 275 K as

$$\Delta S(Q) = S(Q,T) - S(Q,275\ \mathrm{K}). \quad (3)$$

The difference radial distribution function was then calculated by Fourier transformation as

$$\Delta G(r) = \frac{1}{2\pi^2 r\,\rho_0}\int_{Q_{min}}^{Q_{max}} Q\Delta S(Q)\exp(-0.003Q^2)\sin(Qr)\mathrm{d}Q, \quad (4)$$

where ρ_0 denotes the number density, Q_{min} and Q_{max} are the lower and upper limits, respectively, of the momentum transfer Q available in the present experiment.

Quasi-Elastic Neutron Scattering Experiments. Quasi-elastic neutron scattering measurements were performed with two types of inverted geometry TOF spectrometers LAM-40 and LAM-80ET installed at KENS, whose energy resolutions are $\Delta E \approx 200$ and 20 meV, respectively. LAM-40 and LAM-80ET can measure quasi-elastic scattering spectra in the momentum transfer at the elastic position range $0.208 \le Q/\text{Å}^{-1} \le 2.353$ and $0.251 \le Q/\text{Å}^{-1} \le 1.645$ in the energy transfer windows ω/meV ≤ ±10 and ω/meV ≤ ±0.3, respectively. The details of these spectrometers have been described elsewhere.[29,30] The neutron scattering experiments using LAM-40 were made on bulk H_2O at 275, 283, and 295 K and H_2O in Develosils 30 and 100 of $R = 0.97$ and 0.87, respectively, at 243, 258, 275,

and 295 K. Furthermore, high-resolution experiments were carried out on H_2O in Develosil 30 of $R = 0.80$ at 258, 268, and 295 K on LAM-80ET. The bulk water and the silica samples were kept in a doubly walled cylindrical aluminum container of 130 mm height, 14 mm in outer diameter, 0.25 mm thickness, and a sample thickness 0.25 mm to suppress the multiple scattering. The temperature of the sample was measured by a copper−constantan thermocouple and controlled within ±0.5 K. All measurements were started after keeping the sample at a selected temperature for 30 min. The intensity of scattered neutrons was accumulated for about 3 and 6 h on LAM-40 and LAM-80ET, respectively. The spectra of an empty aluminum container and a vanadium tube of 103 mm height, 14 mm diameter, and 0.5 mm thickness were also measured at 295 K for correction of background and normalization to an absolute unit, respectively.

The observed quasi-elastic neutron scattering spectra for bulk H_2O and Develosils 30 and 100 filled with H_2O were corrected for absorption, an aluminum container, the counter efficiency, and the incident neutron spectrum. The contribution from dry Develosil sample was then subtracted from the total scattering data for the Develosil samples by using eq 1 as previously described. The observed differential scattering cross section thus obtained can be approximated to the incoherent dynamical structure factor $S_{inc}(Q,\omega)$ through

$$\frac{\partial^2 \sigma_{inc}}{\partial\Omega\partial E} = \frac{k_1}{k_0}(\langle b^2\rangle - \langle b\rangle^2)\, S_{inc}(Q,\omega), \qquad (5)$$

where k_0 and k_1 are the wave vectors of incident and scattered neutrons, respectively. Q is defined as $Q = k_0 - k_1$. b is the scattering length of hydrogen atom and $4\pi(\langle b^2\rangle - \langle b\rangle^2)$ is the incoherent scattering atomic cross section. In the present analysis, the dynamical structure factor $S_{inc}(Q,\omega)$ was calculated by using eq 5.

The observed dynamical structure factors of bulk H_2O and H_2O in the silica samples were analyzed by a curve-fitting procedure with model functions using the computer programs QUESA40[29] and KIWI,[31] respectively.

Proton NMR Measurements. The dynamcis of water molecules in Develosils 30 and 100 of $R = 1.0$ was studied by an NMR relaxation technique over a temperature range from 208 to 298 K. NMR measurements were carried out on a 200 MHz spectrometer (JEOL JNM-FX200). The temperature of a silica sample was measured with a copper−constantan thermocouple and controlled within ±0.3 K by hot air and/or dry nitrogen stream from liquid nitrogen. Prior to the measurement the sample was left at a selected temperature for about 30 min. The proton spin-lattice relaxation times, T_1, for the silica sample were determined by using both the inversion recovery method (180°-τ-90° pulse sequence) and the saturation recovery method (90°-τ-90° pulse sequence). The spin-spin relaxation times, T_2, were also measured by the Carr−Purcel−Meiboom−Gill method. The half-width at half maximum (HWHM) and the area of proton NMR peak were estimated in the above temperature range.

Results and Discussion

Thermal Behavior. The DSC curves measured for Develosils 30 and 100 filled with H_2O of various R values are shown in Figure 1. In the cooling curves for water in Develosil 30 of $R = 0.86$ and 1.0, two exothermic peaks were observed around 233 and 237 K, whereas no peaks appeared for the sample of $R = 0.45$. For the water in Develosil 100, on the other hand, two exothermic peaks were observed at 231 and 236 K for $R = 0.21$, and a large, sharp exothermic peak was observed at 252 K for $R = 0.91$. For $R = 0.12$, a very small exothermic peak was found at 230 K. These cooling curves show that vitrification of water in the silica pores depend on both pore size and water content. In the heating curves for water in Develosil 30 of $R = 0.96$ and 1.0 and in Develosil 100 of $R = 0.21$ and 0.91, a broad endothermic peak appeared in the temperature range 255−269 K, ascribed to the melting of frozen water.

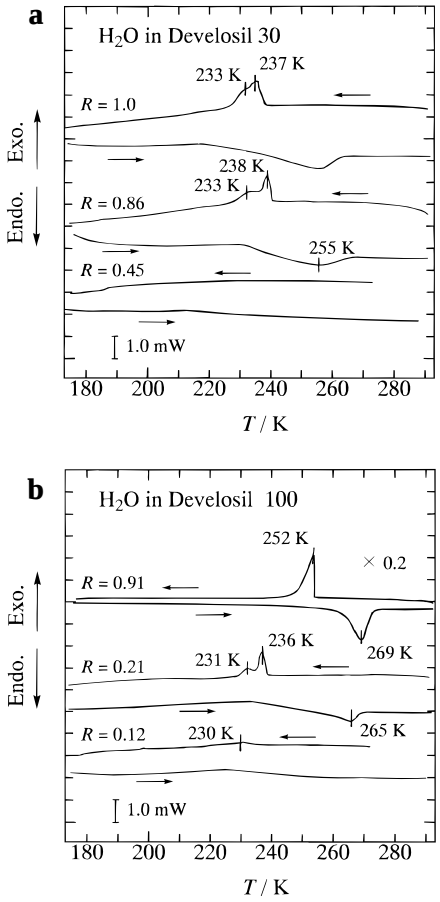

Figure 1. DSC curves for Develosils 30 (a) and 100 (b) samples of various R values. The arrows show the direction of temperature scanning.

TABLE 1: Heat of Freezing Values As Estimated from the Exothermic Peaks in Figure 1

sample	water content, R	peak position, T/K	heat of freezing, kJ mol^{-1}
Develosil	1.0	233, 237	1.17[a]
30	0.86	233, 238	0.82[a]
	0.45		
100	0.91	252	3.35
	0.21	231, 236	1.23[a]
	0.12	230	

[a] The values were the sum estimated from two peaks.

The heats of freezing per mole of water were estimated from the area of the exothermic peaks and are summarized in Table 1. As seen in Table 1, these values obtained for Develosils 30 and 100 are much smaller than the heat of crystallization of bulk water (6.01 kJ mol^{-1}) and decrease with decreasing pore size and water content. These observations suggest that the water close to the pore surface is significantly affected by the silanol groups of the silica. Furthermore, two exothermic peaks observed for water in Develosil 30 of $R = 0.86$ and 1.0 and in Develosil 100 of $R = 0.21$ suggest that there are two types of water in the pores, *i.e.*, one type of water behaves like bulk

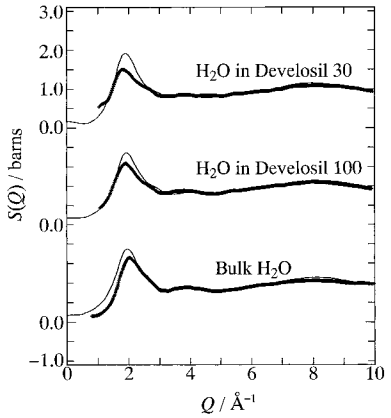

Figure 2. The structure factors $S(Q)$ for D_2O in Develosils 30 and 100 at $R = 1.0$ and for bulk D_2O at 295 K. The experimental values are drawn by crosses and those calculated by a two-state model by solid lines.

water, probably present in the central region of the pores, and the other is water perturbed strongly by the silanol groups on the silica surfaces, freezing at lower temperature. Moreover, it is likely that nonfreezing water is partly present in both Develosils 30 and 100 on the basis of small heat of freezing in Table 1.

It is noteworthy that the thermal behavior of water in Develosil 100 of $R = 0.91$ is apparently different from the other cases in Table 1 in respect of only a large and sharp peak, the largest value of heat of freezing, and the highest temperature of freezing. This result shows that water in the silica pores of 30 and 100 Å of high water content freezes in a different manner.

Neutron Diffraction. First, the structure of water in the silica pores at ambient temperature is compared with that of bulk water. Figure 2 shows the structure factor $S(Q)$ of D_2O in Develosils 30 and 100 of $R = 1.0$ of 295 K, together with that of bulk D_2O for comparison. Apparently, the first peak at 1.9 $Å^{-1}$ in $S(Q)$ for D_2O in Develosil 30 decreases, and the hump centered at 4 $Å^{-1}$ becomes shallower, compared with those for Develosil 100 and bulk. In order to make a semiquantitative analysis on the structure factors, a model fitting approach proposed by Misawa[32] was used, based on a classical two-state model of water, *i.e*. hydrogen-bonded water molecules and randomly orientated water molecules. Although the hydrogen bonding may be defined in more sophisticated, but sometimes complicated, ways in terms of the hydrogen bonding energy, the bond angle, *etc*., the two-state model is still useful to easily understand the characteristics of hydrogen bonding with temperature and pressure. In addition, the present neutron diffraction data are related to both time- and space-averaged structural information and thus do not give the energetic distribution of hydrogen bonding. In the case of the randomly oriented water molecules, the total structure factor $S_0(Q)$ can be expressed as

$$S_0(Q) = f_1(Q) + f_{2U}(Q)[S_{OO}(Q) - 1]. \quad (6)$$

Here, $f_1(Q)$ denotes the form factor of one water molecule written by

$$f_1(Q) = 1 + \frac{4b_O b_D}{3\langle b\rangle^2}\frac{\sin(Qr_{OD})}{Qr_{OD}}\exp\left(-\frac{\langle(\Delta r_{OD})^2\rangle}{2}Q^2\right) + \frac{2b_D^2}{3\langle b\rangle^2}\frac{\sin(Qr_{DD})}{Qr_{DD}}\exp\left(-\frac{(\Delta r_{DD})^2}{2}Q^2\right) \quad (7)$$

with $\langle b\rangle = (b_O + 2b_D)/3$. $f_{2U}(Q)$ represents the form factor for random orientation,

$$f_{2U}(Q) = \frac{1}{3\langle b\rangle^2}\left[b_O + 2b_D\frac{\sin(Qr_{OD})}{Qr_{OD}}\exp\left(-\frac{\langle(\Delta r_{OD})^2\rangle}{2}Q^2\right)\right]^2, \quad (8)$$

where the intramolecular structural parameters[33] are $r_{OD} = 0.934$ Å, $\Delta r_{OD} = 0.138$ Å, $r_{DD} = 1.53$ Å, and $\Delta r_{DD} = 0.24$ Å, and $S_{OO}(Q)$ is the oxygen−oxygen structure factor derived from X-ray scattering.[34]

When N pairs of the nearest-neighbor water molecules form linear hydrogen bonds (LHB), the structure factor $S(Q)$ may be written as

$$S(Q) = S_0(Q) + \Delta S(Q). \quad (9)$$

The second term corresponds to the contribution from the N pairs of water molecules bound by LHB and is given by

$$\Delta S(Q) = N[f_{2C}(Q) - (f_{2U}(Q) - \frac{b_O^2}{3\langle b\rangle^2}F_{OO}(Q)]. \quad (10)$$

Here,

$$F_{OO}(Q) = \frac{\sin(Qr_{OO})}{Qr_{OO}}\exp\left(-\frac{\langle(\Delta r_{OO})^2\rangle}{2}Q^2\right), \quad (11)$$

and

$$f_{2C}(Q) = \sum\sum\frac{b_i b_j}{3\langle b\rangle^2}\frac{\sin(Qr_{ij})}{Qr_{ij}}\exp\left(-\frac{\langle(\Delta r_{ij})^2\rangle}{2}Q^2\right), \quad (12)$$

The fitting results are shown in Figure 2. The discrepancies at $Q = 1.0-2.5$ $Å^{-1}$ may be ascribed to low resolution in Q of the HIT spectrometer. The results of the fits showed that the number of LHB decreases from $N = 3.5$ for bulk D_2O to $N = 2.5$ for D_2O in Develosil 30. The decrease in the number of LHB is probably caused by the silanol groups on the silica surface. This result rationalizes the smaller heat of freezing for water in the pores given in Table 1. It has been found, however, that the nearest-neighbor O−O distance and the orientational correlation of LHB in the pores are not significantly different from those in the bulk. The present results are consistent with both conclusions from the neutron diffraction experiments on the structure of D_2O in pores of 20 Å (Gasil 200) and 90 Å (Spherisorb S20W) by Steytler *et al*.[12] and of 50 Å (Vycor 7930) by Bellissent-Funel *et al*.[22]

Figure 3 shows the difference structure factors, $\Delta S(Q)$, of D_2O in Develosil 30 of $R = 1.0$ measured at 193, 223, 243, and 258 K, which were derived by eq 3 on the basis of the structure factor $S(Q)$ at 275 K. Figure 4 shows the corresponding radial distribution functions obtained by eq 4. As seen in Figure 4, the structure of D_2O in the 30 Å pores is gradually enhanced with decreasing temperature, particularly, below 223 K, the temperature of vitrification. The peak at 1.80 Å is attributable to the intermolecular O···D hydrogen bonds; the peak position does not change significantly with temperature and is similar to that in bulk D_2O.[33] The enhancement of the 1.80 Å peak at 193 K demonstrates an increase in the number of LHB and hence the hydrogen bond network in D_2O in the 30 Å pores. Interestingly, no Bragg peaks have been observed at 193 and 223 K in Figure 3, suggesting that either amorphous ice or an irregular three-dimensional network of ice is formed in the 30 Å pores.

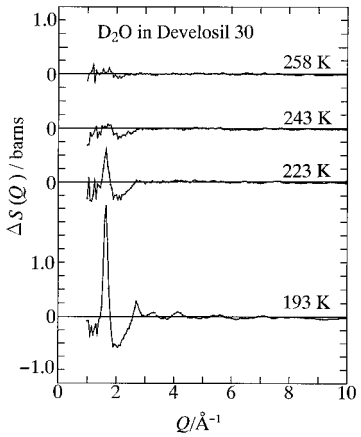

Figure 3. The difference structure factor $\Delta S(Q)$ for D_2O in Develosil 30 with $R = 1.0$ at various temperatures. The experimental values are drawn by dots, and those in the Q region from 1.0 to 3.0 $Å^{-1}$ are connected by solid lines to clarify their variation.

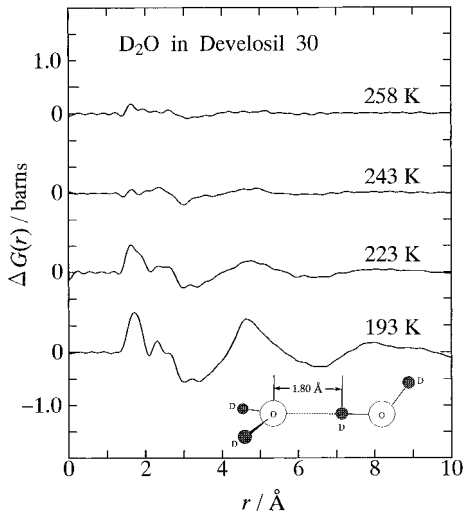

Figure 4. The difference radial distribution curve $\Delta G(r)$ obtained for D_2O in Develosil 30 with $R = 1.0$ at various temperatures.

Figure 5 shows the structure factors $S(Q)$ of D_2O in Develosil 100 of $R = 0.76$ in a temperature range from 213 to 295 K and of bulk D_2O at 213 K. As seen in Figure 5, the Bragg patterns due to crystallization of D_2O appear for the 100 Å pores below 238 K, in contrast with the patterns for water in the 30 Å pores. The lattice spaces, d, were estimated from the Bragg peaks both for D_2O in the 100 Å pores and for bulk D_2O at 213 K and are summarized in Table 2, together with those of ice I_h and I_c taken from the literature.[35] It is apparent from the assignment of the Bragg patterns that ice I_c is formed in the 100 Å pores, while ice I_h crystallizes in the bulk. The present results agree with that obtained in neutron diffraction studies on D_2O in Spherisorb S20W of the pore size 90 Å by Dore *et al.*[15] and in Vycor 7930 of the pore size 50 Å by Bellissent-Funel *et al.*[22] However, the phase transition from I_h to I_c reported at 252 K in Spherisorb S20W[15] was not confirmed in the present study. It is well known that ice I_c is obtained in heating of microparticles of amorphous water, made on a wall of the vessel by aggregation of water vapor below 113 K. It is likely that a similar phase transformation to ice I_c with temperature occurs in Develosil 100 because the long-range ordering of water is perturbed in the pores by the silanol groups as in the case of amorphous water. The crystallization of ice I_c in the 100 Å pores would be explainable from different crystal structures of ice I_h and I_c as follows. A unit ring of six water molecules like a chair-formed cyclohexane molecule is formed in both ice structures.

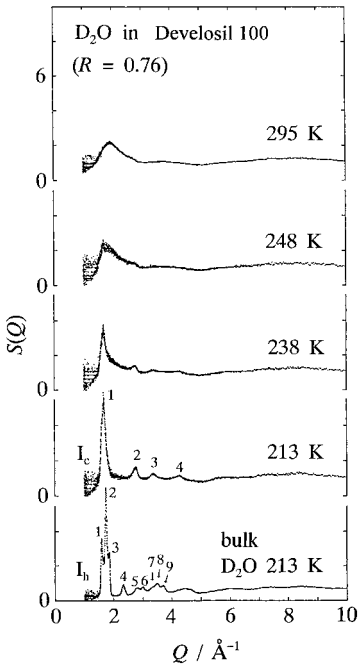

Figure 5. The structure factor $S(Q)$ for D_2O in Develosil 100 with $R = 0.76$ at various temperatures and for pure D_2O ice at 213 K.

TABLE 2: Lattice Space (d/Å) Observed for D_2O in Develosil 100 and in Bulk Water at 213 K in Figure 5, and for Ice I_h and I_c (ref 35)

	D_2O	D_2O	ice			
No.	in silica	in bulk	I_h	(hkl)	I_c	(hkl)
1	3.70	3.93	3.90	100	3.68	111
2	2.30	3.59	3.66	002	2.25	220
3	1.80	3.40	3.40	101	1.92	311
4	1.46	2.67	2.67	102	1.59	400
5		2.23	2.25	110	1.46	331
6		2.10	2.07	103	1.30	422
7		1.86	1.95	200	1.22	333
8		1.79	1.92	112		
9		1.70	1.89	201		
			1.72	202		
			1.52	203		

In the structure of ice I_h, the units are connected by hydrogen bonds to form an uneven sheet in the *ab*-plane. Furthermore, the sheets are stacked to form a three-dimensional structure having the six-membered cavities along the *c*-axis. On the other hand, ice I_c has the diamond type structure, *i.e.*, the three-dimensional structure does not consist of the stacking of the uneven sheets formed in ice I_h. In the crystallization of water in the 100 Å pores, the diamond type structure is probably more favored than the stacking structure of the widespread sheets because of the very narrow space in the pores and the effect of the silanol groups.

The different thermal behaviors of water in Develosils 30 and 100 observed by the DSC experiments are now understood in terms of the microscopic structures from the present neutron diffraction experiments. The exothermic peaks observed at around 233 and 237 K in cooling water in the 30 Å pores is attributed to the formation of randomly or amorphous ice, whereas the large and sharp peak at 252 K in the cooling curve for the 100 Å pores arises from the crystallization of ice I_c in the pores. These findings certainly suggest the presence of more bulk water in the 100 Å pores than in the 30 Å pores.

Quasi-Elastic Neutron Scattering. Six quasi-elastic neutron scattering spectra in the Q-range 0.621−2.353 $Å^{-1}$ were measured simultaneously by six detectors with the LAM-40 spectrometer at selected temperatures from 243 to 295 K for

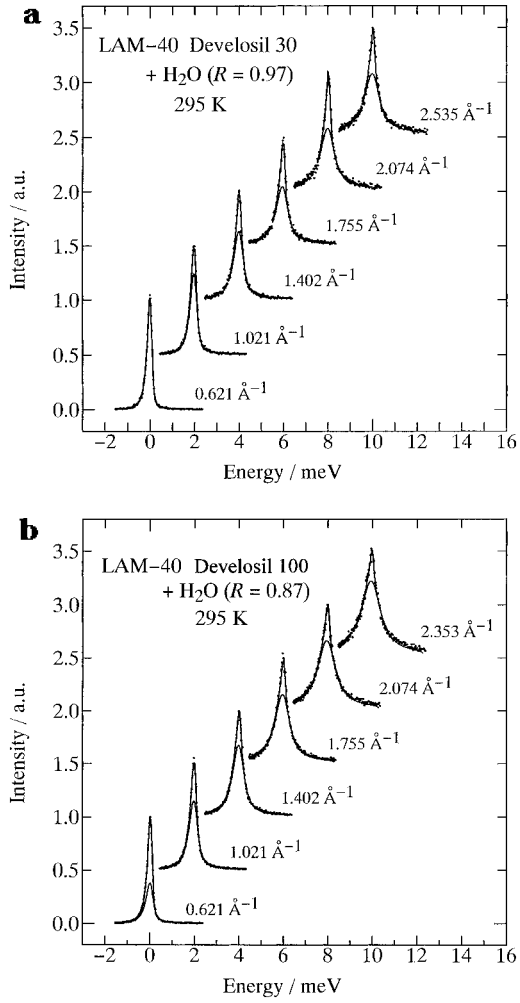

Figure 6. The Q-dependence of quasi-elastic neutron scattering spectra by LAM-40 spectrometer in the scattering factor range 0.621−2.353 Å^{-1} for H_2O in Develosils 30 (a) and 100 (b) at $R = 0.97$ and 0.87, respectively, at 295 K. Experimental values are drawn by dots and calculated by solid lines.

bulk H_2O and H_2O in Develosils 30 and 100 of $R = 0.97$ and 0.87, respectively.

Figures 6, parts a and b, show typical spectra at 295 K measured for H_2O in Develosils 30 and 100, respectively. The observed values for bulk H_2O and the silica samples were analyzed in a least-squares procedure. The scattering law used in the analysis for the silica samples may be given by

$$S(Q,\omega) = C\left[\frac{A_n}{\pi}\frac{\Gamma_n}{\omega^2+\Gamma_n^2} + \frac{A_b}{\pi}\frac{\Gamma_b}{\omega^2+\Gamma_b^2} + (1-A_n-A_b)\delta(\omega)\right], \quad (13)$$

where C is a constant, Γ_i ($i = n$ and b) are the half-width at half-maximum (HWHM) of narrow and broad Lorentzian components, respectively, A_i is the fraction of the individual Lorentzians, and $\delta(\omega)$ is a δ-function ascribed to the coherent component. On the other hand, only two Lorentzians were used as the model scattering law in the analysis of bulk H_2O data. The narrow component of the Lorentzians is ascribed to the mean translational motion of water molecules in the bulk and in the silica pores. The broad component was concerned with an inelastic background in the present study. The narrow component was quantitatively analyzed to investigate the mean translational motion of water molecules in the bulk and in the silica pores.

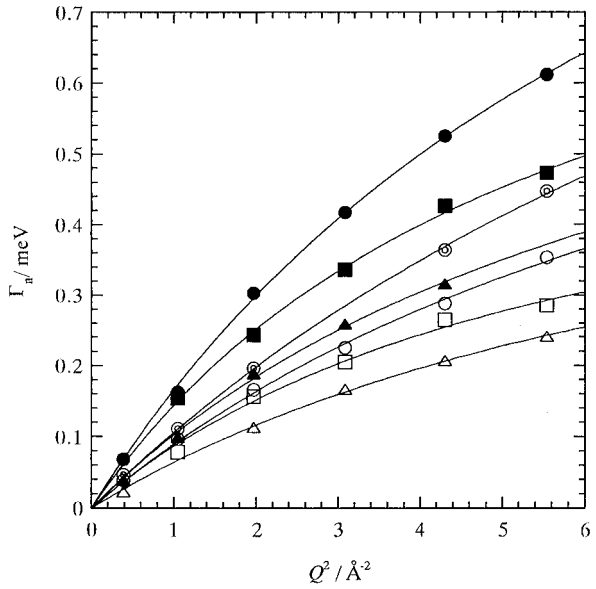

Figure 7. The Q^2-dependence of HWHM on the quasi-elastic narrow component Γ_n for pure H_2O (circle), and H_2O in Develosils 30 (triangle) and 100 (square) at $R = 0.97$ and 0.87, respectively, from LAM-40 experiments at 275 (opened symbol), 283 (doubled symbol), and 295 K (filled symbol). Values fitted with the jump diffusion model are drawn by solid lines.

TABLE 3: The Values of Self-Diffusion Coefficients Estimated by LAM-40 and LAM-80ET Experiments[a]

sample	T/K	$10^{10}\ D_H$/m^2 s^{-1}	spectrometer
bulk water	295	28(1)	LAM-40
	283	17(5)	LAM-40
	275	15(8)	LAM-40
Develosil 30	295	17(2)	LAM-40
($R = 0.97$)	275	10(1)	LAM-40
Develosil 30	295	14(4)	LAM-80ET
($R = 0.80$)	268	6.2(1)	LAM-80ET
	258	5.4(5)	LAM-80ET
Develosil 100	295	26(1)	LAM-40
($R = 0.87$)	275	16(1)	LAM-40

[a] The values in parentheses are their standard deviations.

The HWHMs of the narrow component, Γ_n, obtained for bulk H_2O and H_2O in the silica pores at 275, 283, and 295 K were plotted against the Q^2 values in Figure 7. Apparently, the Γ_n value at 295 K at each Q decreases in the sequence of bulk H_2O > H_2O in the 100 Å pores > H_2O in the 30 Å pores; this result suggests that the mean translational motion of water molecules in the 30 Å pores is most hindered among these three samples. The $Q^2 - \Gamma_n$ data were fitted by using a proton jump diffusion model. The mean proton self-diffusion coefficients obtained are summarized in Table 3. As seen in Table 3, the D_H value (28×10^{-10} m^2 s^{-1}) for bulk H_2O at 295 K obtained on LAM-40 is comparable well with that (21.4×10^{-10} m^2 s^{-1}) determined by the NMR relaxation method[36] and that (23×10^{-10} m^2 s^{-1}) obtained from the neutron scattering experiment by Bellissent-Funel *et al.*[23a] In the case of H_2O in the silica pores, the D_H values (26×10^{-10} and 16×10^{-10} m^2 s^{-1}) obtained for H_2O in the 100 Å pores at 295 and 275 K are also comparable with those (24.3×10^{-10} and 14.3×10^{-10} m^2 s^{-1}) determined for H_2O in Vycor glass (50 Å pores) of $R = 1.00$ and at 298 and 278, respectively.[23a] The comparison demonstrates the reliability of the present LAM-40 experiments and analyses. The D_H value (17×10^{-10} m^2 s^{-1}) at 295 K for the 30 Å pores is significantly smaller than that for bulk. On the contrary, the D_H value (26×10^{-10} m^2 s^{-1}) at 295 K for the 100 Å pores is slightly smaller than that for bulk and is about 1.5 times larger than that for the 30 Å pores. These results

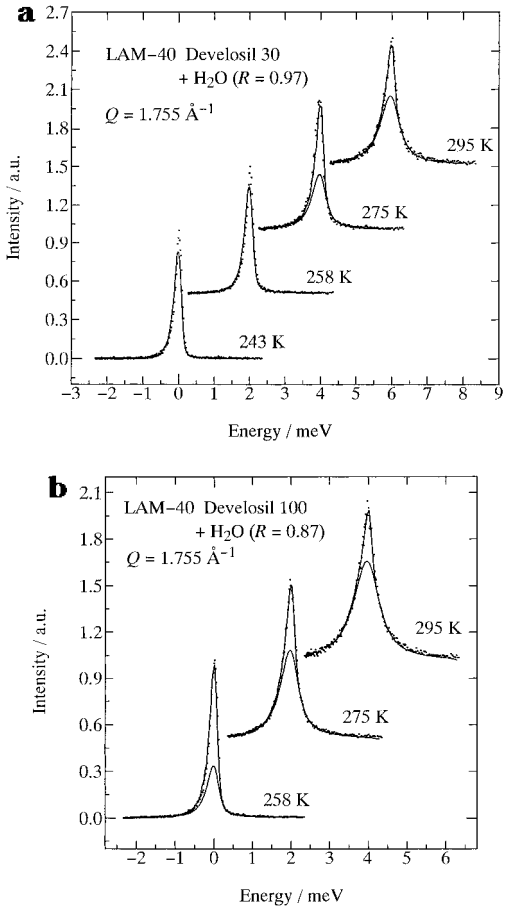

Figure 8. The temperature dependence of quasi-elastic neutron scattering spectra by LAM-40 spectrometer at $Q = 1.755$ Å^{-1} for H_2O in Develosils 30 (a) and 100 (b) at $R = 0.97$ and 0.87, respectively. Experimental values are drawn by dots and calculated by solid lines.

reveal that the motion of water molecules in the 30 Å pores is strongly affected by the silanol groups and that there is more bulk water in the 100 Å pores than in the 30 Å pores.

The temperature dependence of the dynamic property of water molecules in the pores is discussed on the basis of the quasi-elastic neutron scattering data. Figures 8, parts a and b, show the quasi-elastic neutron scattering spectra obtained with LAM-40 at $Q = 1.755$ Å^{-1} for H_2O in 30 and 100 Å pores, respectively. It is apparent that with lowering temperature from 295 to 275 K the neutron scattering spectra for H_2O in both pore sizes sharpen, *i.e.*, the Γ_n values at each Q for every sample decrease as in Figure 7. The D_H values obtained are given in Table 3 and decrease with decreasing temperature from 295 to 275 K; 28×10^{-10} to 15×10^{-10} m^2 s^{-1} for bulk, 17×10^{-10} to 10×10^{-10} m^2 s^{-1} in the 30 Å pores, and 26×10^{-10} to 16×10^{-10} m^2 s^{-1} in the 100 Å pores. These changes in D_H values with temperature show that the translational motion of water molecules in bulk and the silica pores is gradually retarded with decreasing temperature. A difference between the D_H values at 295 and 275 K decreases in the order of 13×10^{-10} m^2 s^{-1} for bulk > 10×10^{-10} m^2 s^{-1} in the 100 Å pores > 7×10^{-10} m^2 s^{-1} in the 30 Å pores, suggesting that the translational motion of water molecules is more rapidly restricted in this order with decreasing temperature. The dynamic property of water molecules in the pores is consistent with their thermodynamic behavior and static structure obtained from previous DSC and neutron diffraction experiments. A quantitative analysis could not be performed on the data obtained below 273 K because of the resolution limit of the LAM-40 spectrometer in a low Q region <1 Å^{-1}.

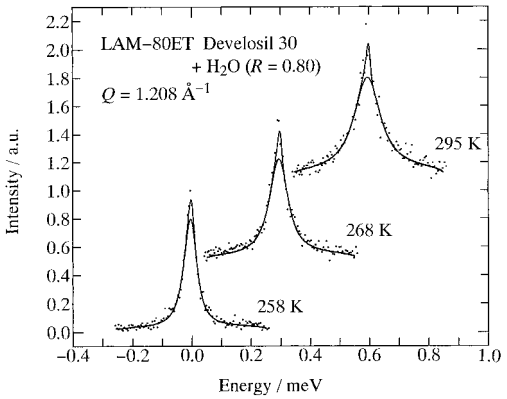

Figure 9. The temperature dependence of quasi-elastic neutron scattering spectra by LAM-80ET spectrometer at $Q = 1.208$ Å^{-1} for H_2O in Develosil 30 at $R = 0.80$. Experimental values are drawn by dots and calculated by solid lines.

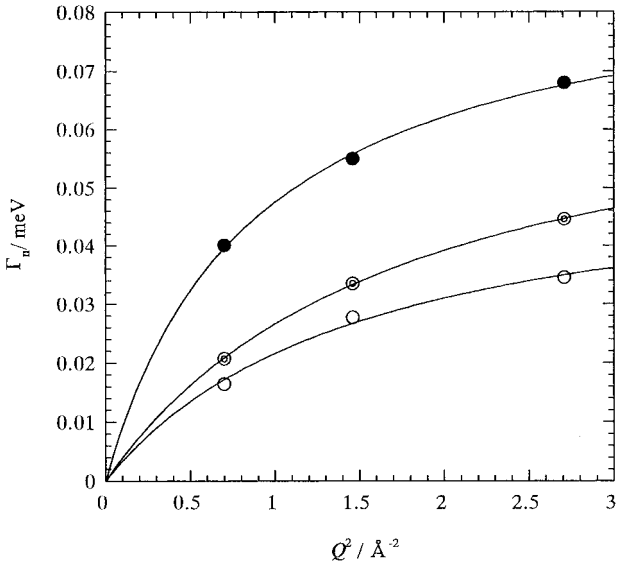

Figure 10. The Q^2-dependence of HWHM on the quasi-elastic narrow component Γ_n for H_2O in Develosil 30 at $R = 0.80$ from LAM-80ET experiments at 258 (opened circle), 268 (doubled circle), and 295 K (filled circle). Values fitted with the jump diffusion model are drawn by solid lines.

High resolution experiments on LAM-80ET were performed on H_2O in Develosil 30 ($R = 0.80$) at 258, 268, and 295 K. Three quasi-elastic neutron scattering spectra at $Q = 0.837$, 1.208, and 1.645 Å^{-1} were simultaneously obtained. Figure 9 shows a temperature dependence of the neutron scattering spectra obtained at $Q = 1.208$ Å^{-1}. The observed values were analyzed by eq 13. As seen in Figure 9, the spectra for H_2O in the 30 Å pores sharpen with lowering temperature. The Γ_n values at 258, 268, and 295 K were plotted against the Q^2 values in Figure 10 and analyzed with the proton random diffusion model. The D_H values obtained are listed in Table 3. As is seen in Table 3, the D_H values (14×10^{-10} m^2 s^{-1}) for the 30 Å pores at 295 K obtained with LAM-80ET is slightly smaller than that (17×10^{-10} m^2 s^{-1}) with LAM-40. One of the reasons for the difference in D_H with the two spectrometers may be due to the different water contents in Develosil 30 samples, $R = 0.97$ (LAM-40) and 0.80 (LAM-80ET) since there is less bulk water at the lower water content in the pores. Another reason is that a high-resolution spectrometer observes mainly the slower motion of water molecules hindered on the silica surfaces than a low-resolution spectrometer does.

As is seen in Table 3, with decreasing temperature the D_H value for the 30 Å pores obtained with LAM-80ET decreases

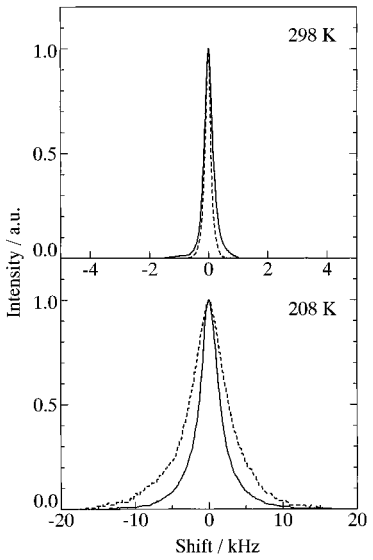

Figure 11. The NMR spectra of H_2O in Develosils 30 (solid lines) and 100 (dashed lines) at 298 (top) and 208 K (bottom). The peak height is normalized to unity.

gradually from 14×10^{-10} at 295 K to 5.4×10^{-10} m^2 s^{-1} at 258 K, demonstrating that the translational motion of water molecules in the 30 Å pores is more hindered at low temperature. Moreover, it is interesting to note that a difference of the D_H values (8.6×10^{-10} m^2 s^{-1} at 295 and 258 K) for the 30 Å pores is smaller than the corresponding value (13×10^{-10} m^2 s^{-1} at 295 and 275 K) for bulk. This result suggests that the temperature effect on translational motion of water molecules is less in the 30 Å pores than in bulk, consistent with those from the DSC and the neutron diffraction experiments previoustly described.

Proton NMR Relaxation. The NMR spectra of H_2O in the 30 and 100 Å pores at 298 and 208 K, which are the highest and the lowest temperatures measured, are shown in Figure 11. The peak width for H_2O in the 100 Å pores at 298 K is narrower than that for the 30 Å pores, suggesting that the motions of water molecules in the 100 Å pores at 298 K are faster than those in the 30 Å pores.

The peak for H_2O in both pores becomes considerably broad as the temperature is lowered. In contrast to at 298 K, the peak width for H_2O in the 100 Å pores at 208 K is broader than that for the 30 Å pores. This finding reveals that the motions of water molecules in the 100 Å pores are more restricted than those in the 30 Å at undercooled temperature.

In order to make more clearly the temperature dependence of the motions of water molecules in the pores, some NMR parameters obtained at the various temperatures were plotted against the temperature. Figure 12, parts a and b, show the temperature dependence of the reciprocal of proton spin-lattice relaxation times, T_1, and of the peak area relative to that at 298 K. Figure 13, parts a and b, show the temperature dependence of the reciprocal of the spin-spin relaxation times, T_2, and of the HWHM of the peak. The T_1 and T_2 data are correlated with the translational and the rotational motions of water molecules in the pores.[37] Both T_1 and T_2 values for H_2O in the 30 and 100 Å pores at $R = 1.0$ reveal that above 253 K the motions of water molecules in the 100 Å pores are faster by a factor 2−3 than those in the 30 Å pores; this result is in agreement with that from the quasi-elastic neutron scattering measurements.

The effect of temperature on the dynamics of water molecules in the pores is observed more clearly in the NMR data than the

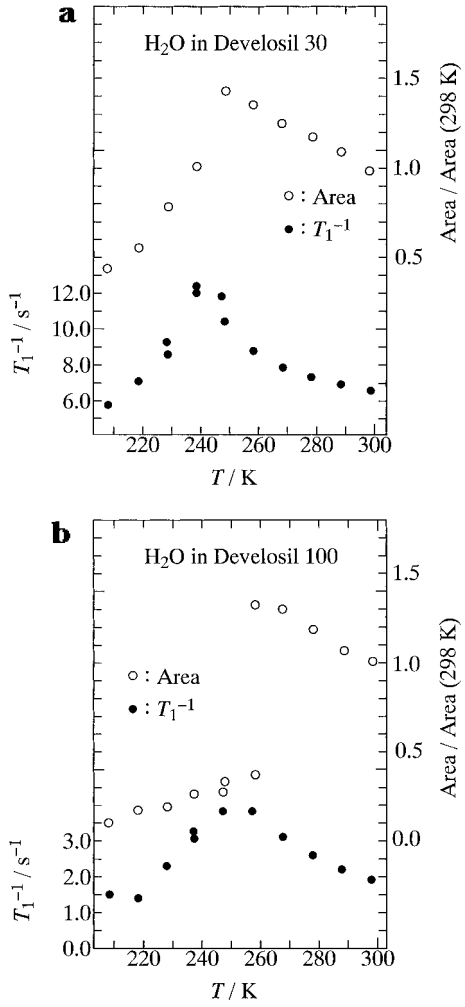

Figure 12. The temperature dependence of the reciprocal of the proton spin-lattice relaxation time T_1 (filled circle) and of the area of the proton NMR peak normalized by the values at 298 K (opened circle) for H_2O in Develosil 30 (a) and 100 (b) at $R = 1.0$.

neutron scattering data. As is seen in Figures 12 and 13, the discontinuities in all the parameters for the 30 and 100 Å pores are observed at around 238 and 253 K, respectively, close to the characteristic temperatures for the exothermic peaks in the DSC curves (Figure 1). In addition, as shown in Figure 12, the decrease in the peak area at 253 K for the 100 Å pores is more marked than that at 238 K for the 30 Å pores. This suggests that the motion of water molecules is restricted more rapidly in the 100 Å pores than in the 30 Å pores with decreasing temperature and that a larger amount of water is frozen in the 100 Å pores than in the 30 Å pores. These results from the NMR data may reflect the different manner of crystallization of water in the 30 and 100 Å pores. With further lowering of the temperature below the point of crystallization, the reciprocal of the T_1 values for both pores gradually decreases, showing that the motion of the water molecules is further restricted with increasing crystallization in the pores. This result agrees well with the conclusion from neutron scattering experiments on D_2O in Vycor 7930 of the pore size 50 Å by Bellissent-Funel *et al.*;[22] they identified the presence of a small amount of liquid water in the pores below the point of crystallization of ice I_c.

Conclusions

The neutron diffraction data for D_2O in Develosils 30 and 100 at ambient temperature have shown that the hydrogen bond

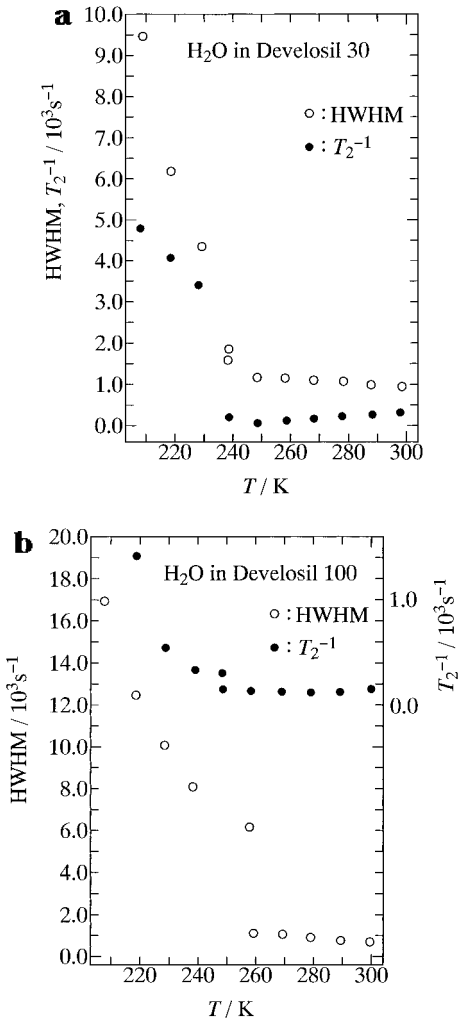

Figure 13. The temperature dependence of the reciprocal of proton spin−spin relaxation time T_2 (filled circle) and of the HWHM of proton NMR peak (opened circle) for H_2O in Develosils 30 (a) and 100 (b) at $R = 1.0$.

distance and the orientation of the neighboring water molecules in the pores are not significantly different from those in bulk. However, the proton self-diffusion coefficients, as determined at 275 and 295 K by quasi-elastic neutron scattering, indicate that the translational motion of the water molecules is hindered in the order of 30 Å pores > 100 Å pores > bulk. This fact probably arises from strong hydrogen bonds between the water molecules and the silanol groups at the silica surfaces. Actually, the number of hydrogen-bonds between the water molecules decreases from ∼3.5 in bulk water to ∼2.5 in the pores. The dynamic data obtained from the proton NMR experiments have revealed that above the freezing point of water the motion of water molecules in the 30 Å pores is more restricted than in the 100 Å pores. This suggests again that the dynamic properties of water molecules in the pores are affected by the silanol groups at the silica surface.

At undercooled temperatures the hydrogen bonds between water molecules in the silica pores are strengthened. However, normal three-dimensional networks of water cannot be easily formed in both pores because of strong interaction of water molecules with silanol groups.

Thus, crystalline ice is not formed in the 30 Å pores, whereas ice I_c is crystallized around 252 K in the 100 Å pores. These changes in phases of water in the pores are reflected on the characteristic exothermic peaks in the DSC curves. With decreasing temperature the motion of water molecules is more quickly hindered in the 100 Å pores than in the 30 Å pores. These dynamic properties of water in the pores are consistent with their static structures at undercooled temperatures.

The present study suggests that the hydrogen-bonds between water molecules and silanol groups play an important role in various behaviors of water in porous silica. In particular, the dynamics of water molecules in the pores is more sensitive to the silanol groups than the static structures. These conclusions will aid in the understanding chemical reactions in porous materials such as zeolites and ion exchange resins, and furthermore, the structure and dynamic properties of nonfreezing water in biological cells.

Acknowledgment. The authors are grateful to Prof. T. Inoue of Fukuoka University for the use of the differential scanning calorimeter and Mr. H. Fujii of Fukuoka University for his help in the analyses of the neutron quasi-elastic scattering data. The authors are also grateful to the members of HIT and LAM groups for valuable assistance during the measurements. The authors are grateful to Prof. T. Kanaya of Kyoto University, Dr. T. Kamiyama of Hokkaido University, and Prof. Y. Izumi of Yamagata University for providing the programs for QUESA40, KIWI, and absorption correction and for valuable discussion on the results from the LAM-40 and LAM-80ET experiments. All calculations were performed at the Computer Center of Fukuoka University.

References and Notes

(1) Clifford, J. In *Water, A Comprehensive Treatise*; Franks, F., Ed.; Plenum: New York, 1975; Vol. 5, Chap. 2.
(2) Franks, F. In *Water, A Comprehensive Treatise*; Franks, F., Ed.; Plenum: New York, 1980; Vol. 7, Chap. 3.
(3) Stillinger, F. H. In *Water in Polymers*; Rowland, S. P., Ed.; Washington, DC, 1980; pp 11−21.
(4) Babkin, Y.; Kiselev, A. V. *Russ. J. Phys.* **1963**, *37*, 118.
(5) Davydov, V. Y.; Kiselev, A. V.; Lokutsievskii, V. A.; Lygin, V. I. *Russ. J. Phys. Chem.* **1974**, *48*, 1342.
(6) Mills, R.; Morariu, V. V. *Z. Phys. Chem. (Frankfurt am Main)* **1972**, *79*, 1.
(7) Klier, K.; Zettlemoyer, A. C. *J. Colloid Interface Sci.* **1977**, *58*, 216.
(8) McTague, J. P.; Nielson, M.; Passell, L. *Crit. Rev. Solid State Mater. Sci.* **1978**, *8*, 135.
(9) Hall, P. G.; Pidduck, A. J.; Wright, C. J. *J. Colloid Interface Sci.* **1981**, *79*, 339.
(10) Hall, P. G.; Williams, R. T.; Slade, R. C. T. *J. Chem. Soc., Faraday Trans. 1* **1985**, *81*, 847.
(11) Clark, J. W.; Hall, P. G.; Pidduck, A. J.; Wright, C. J. *J. Chem. Soc., Faraday Trans. 1* **1985**, *81*, 2067.
(12) Steytler, D. C.; Dore, J. C.; Wright, C. J. *Mol. Phys.* **1983**, *48*, 1031.
(13) Steytler, D. C.; Dore, J. C.; Wright, C. J. *J. Phys. Chem.* **1983**, *87*, 2458.
(14) Steytler, D. C.; Dore, J. C. *Mol. Phys.* **1985**, *56*, 1001.
(15) Dore, J. C.; Dunn, M.; Chieux, P. *J. Phys. Coll. C1, supplement 3* **1987**, *48*, 457.
(16) Gerasimowicz, W. V.; Garroway, A. N.; Miller, J. B.; Sander, L. C. *J. Phys. Chem.* **1992**, *96*, 3658.
(17) Bosio, L.; Johari, G. P.; Oumezzine, M.; Teixeira, J. *Chem. Phys. Lett.* **1992**, *188*, 113.
(18) Katayama, S.; Fujiwara, S. *J. Phys. Chem.* **1980**, *84*, 2320.
(19) Murase, N.; Gonda, K.; Watanabe, T. *J. Phys. Chem.* **1986**, *90*, 5420.
(20) Tsutsumi, K.; Mizoe, K. *Colloids Surfaces* **1989**, *37*, 29.
(21) Yamada-Nosaka, A.; Ishikiriyama, K.; Todoki, M.; Tanzawa, H. *J. Appl. Polym. Sci.* **1990**, *39*, 2443.
(22) Bellissent-Funel, M.-C.; Lal, J.; Bosio, L. *J. Chem. Phys.* **1993**, *98*, 4246.
(23) (a) Bellissent-Funel, M.-C.; Bradley, K. F.; Chen, S. H.; Lal, J.; Teixeira, J. *Physica A* **1993**, *201*, 277. (b) Bellissent-Funel, M.-C.; Chen, S. H.; Zanotti, J.-M. *Phys. Rev. E* **1995**, *51*, 4558.
(24) Hansen, E. W.; Stöcker, M.; Schmidt, R. *J. Phys. Chem.* **1996**, *100*, 2195.

(25) (a) Watanabe, N.; Fukunaga, T.; Shinohe, T.; Yamada, K.; Mizoguchi, T. In *Proceedings of the 4th International Collaboration on Advanced Neutron Sources* (ICANS-IV), KEK, Tsukuba, Oct 20−24, 1980; Ishikawa, Y. *et al*., Eds.; National Laboratory for High Energy Physics: Tsukuba, 1981; p 539. (b) Misawa, M.; Fukunaga, T.; Yamaguchi, T.; Watanabe, N. In *Proceedings of the 9th International Collaboration on Advanced Neutron Sources* (ICANS-X), SIN, Villigen, Sept. 22−26, 1986; Atchison, F.; Fischer, W.,Ed.; Swiss Institute for Nuclear Research: Villigen, 1987; p 539.

(26) Paalman, H. H.; Pings, C. J. *J. Appl. Phys.* **1962**, *33*, 2635.

(27) Soper, A. K.; Egelstaff, P. A. *Nucl. Instrum. Methods* **1980**, *178*, 415.

(28) Sears, V. F. In *Thermal-Neutron Scattering Lengths and Cross Sections for Condensed-Matter Research*; Chalk River Lab.: Ontario, 1984.

(29) Inoue, K.; Ishikawa, Y.; Watanabe, N.; Kaji, K.; Kiyanagi, Y.; Iwasa, H.; Kohgi, M. *Nucl. Instrum. Methods* **1984**, *A238*, 401.

(30) Inoue, K.; Kanaya, T.; Kiyanagi, Y.; Ikeda, S.; Shibata, K.; Iwasa, H.; Kamiyama, T.; Watanabe, N.; Izumi, Y. *Nucl. Instrum. Methods* **1991**, *A309*, 294.

(31) A fit program for quasi-elastic data analysis, "KIWI ver.1.01" made by Fanjat, N.

(32) Yamaguchi, T.; Tamura, Y.; Ohtaki, H.; Ikeda, S.; Misawa, M. *KENS Rep*. (National Laboratory for High Energy Physics, Tsukuba, Japan) **1986**, *6*, 125.

(33) Narten, A. H. *J. Chem. Phys.* **1972**, *56*, 5681.

(34) Narten, A. H.; Levy, H. A. *J. Chem. Phys.* **1971**, *55*, 2263.

(35) Berry, L. G., Ed. In *Powder Diffraction File Sets 16 to 18*; Inorganic Volume No. PD1S-18iRB; Joint Committee on Powder Diffraction Standards: Pennsylvania, 1974.

(36) Wang, J. H. *J. Am. Chem. Soc.* **1951**, *73*, 510.

(37) Lang, E. W.; Lüdemann, H.-D., Ed. In *NMR Basic Principles and Progress*; Springer-Verlag: Berlin, 1990; Vol. 24, pp 130−187.